Chemical Engineering Journal 163 (2010) 93–97

Contents lists available at ScienceDirect

Chemical Engineering Journal

journal homepage: www.elsevier.com/locate/cej

Catalytic synthesis of diethyl carbonate by oxidative carbonylation of ethanol over $PdCl_2$/Cu-HMS catalyst

Pingbo Zhang[a,b,*], Xinbin Ma[a]

[a] Key Laboratory for Green Chemical Technology, School of Chemical Engineering and Technology, Tianjin University, Tianjin 300072, PR China
[b] School of Chemical and Material Engineering, Jiangnan University, Wuxi 214122, PR China

ARTICLE INFO

Article history:
Received 30 January 2010
Received in revised form 29 June 2010
Accepted 9 July 2010

Keywords:
Diethyl carbonate
Oxidative carbonylation
Cu-HMS
Si/Cu

ABSTRACT

Direct synthesis of diethyl carbonate (DEC) by oxidative carbonylation of ethanol offers a prospective "green chemistry" strategy to eliminate the phosgene used in the traditional preparation processes. $PdCl_2$/Cu-HMS catalyst has been investigated, which demonstrated excellent selectivity to DEC by oxidative carbonylation of ethanol in the gas-phase reaction. The Si/Cu molar ratio of mesoporous Cu-HMS supports showed a remarkable effect on catalytic activities. An optimized Si/Cu molar ratio existed for catalytic performance, which was about 50/1. From XPS, ICP, XRD, nitrogen physisorption and IR characterization and analysis, it could be concluded that copper species incorporated into HMS frame and was highly dispersed in the frame of silica. The catalytic performances of $PdCl_2$/Cu-HMS were related with both Cu content in the Cu-HMS and the order degree of mesoporous structure for Cu-HMS.

1. Introduction

Diethyl carbonate (DEC) is recognized as an environmentally benign chemical because of its negligible ecotoxicity and low bioaccumulation and persistence. Because of its high oxygen contents (40.6 wt.%), DEC has been proposed as a replacement for *tert*-butyl ether (MTBE) [1] as an attractive oxygen-containing fuel additive. A further significant advantage of DEC over other fuel oxygenates such as MTBE is that DEC could slowly decompose to CO_2 and ethanol, which have no environmental impact when released into the environment [2]. In addition, the gasoline/water distribution coefficients for DEC are more favorable than those for dimethyl carbonate (DMC) and ethanol [3]. Besides these applications as a fuel additive, DEC is also drawing attention as a safe solvent and an additive in lithium cell electrolyte [3–5].

Several synthetic routes to DEC have been developed so far, e.g., (i) the phosgene–ethanol process, in which $COCl_2$ is reacted with ethanol, obviously involving dangerous phosgene gas [6]; (ii) the oxidative carbonylation of ethanol over a slurry of CuCl [7]; (iii) reaction between ethyl nitrite (C_2H_5ONO) and carbon monoxide [8]; (iv) the gas-phase oxidative carbonylation of ethanol using a heterogeneous catalyst [9–12]; (v) transesterification reaction of DMC and ethanol [13,14]; (vi) activation of carbon dioxide [15]; (vii) reaction of ethanol with urea over organotin catalysts [16]. Among them, oxidative carbonylation of ethanol in the gas-phase has been deemed as one of the most promising routes for DEC synthesis based on the "green chemistry" principles [1,9]. Also, it is well known that the structures and component of support play an important role in the structures and activities of supported catalysts. Since 1980s, efforts have been made in the development of supported copper-based catalysts for DMC synthesis. All kinds of catalysts were prepared by impregnating the active carbon, oxides (MnO, ZnO, TiO_2, SiO_2, and Al_2O_3) or HMS silica in methanol solution of $CuCl_2$ [9,17]. Previous results have shown that all of the tested catalysts deactivated quickly because of losing the chlorine anion and the remodel of active copper species on the surface. Recently, HY zeolite and mesoporous MCM-41 silica have been reported as the promising supports for the oxidative carbonylation reaction [18–22], wherein CuY catalyst and CuCl/MCM-41 catalyst were prepared by the high temperature solid state ion-exchange method. However, in the case of synthesis of DEC by oxidative carbonylation, only active carbon was widely used as the support. Hence, efforts have been dedicated to develop more suitable supports than active carbon for more efficient gas-phase oxidative carbonylation of ethanol to DEC. And it turns out to be highly interesting to further explore the other possible applications of the catalytically attractive materials for DEC synthesis. In our previous work, it mainly reported a new type of catalyst and illuminated the catalytic reaction mechanism by the interaction between Pd^{2+} loaded on the surface and Cu^{2+} in Cu-HMS frame [23]. This report is the continuation of that work.

This paper mainly made further investigation on the structural properties of Cu-HMS on the DEC synthesis. It was found that a

* Corresponding author at: School of Chemical and Material Engineering, Jiangnan University, Wuxi 214122, PR China.
E-mail address: pingbozhang@gmail.com (P. Zhang).

1385-8947/$ – see front matter © 2010 Elsevier B.V. All rights reserved.
doi:10.1016/j.cej.2010.07.025

reasonable amount of $PdCl_2$ loadings was a critical point in the DEC preparation. In addition, the effects of Si/Cu molar ratio of $PdCl_2$/Cu-HMS catalysts on the reaction performances for producing DEC were investigated.

2. Experimental

2.1. Catalyst preparation

The HMS and Cu-HMS were synthesized following the procedures similar to those proposed by Tanev et al. via a neutral templating pathway using dodecylamine (DDA) as a surfactant [24,25]. In a typical synthesis, 3.85 g of DDA was dissolved in 130 ml of water, 32.5 ml of ethanol was then added to generate a 40:10 H_2O/EtOH solution of the surfactant. The surfactant solution was stirred for 15 min. At the same time, 0.35 g of copper chloride was added in the mixture of 20 ml ethanol and 23 ml tetraethyl orthosilicate (TEOS). Then the mixture was slowly added to the surfactant solution, stirred for about 2 h. The resultant solution was aged for 18 h at room temperature (25 °C) to obtain crystalline products. The solid precipitates were filtered out, dried at 120 °C over night, and calcined at 600 °C for 4 h. Finally, Cu-HMS was obtained for further experiments.

A Pd-containing solution was prepared by heat-dissolving palladium chloride ($PdCl_2$) in methanol solution at a temperature of 65 °C. Fully dried Cu-HMS supports were mixed with the solution and was then stirred for about 3 h to impregnate the Cu-HMS with Pd-containing solution. Thereafter, methanol was evaporated away from the mixture at a temperature of 65 °C under a reduced pressure. The residual mixture was heat-treated at 120 °C for 1 h to get a solid catalyst. The total contents of the metal compound in terms of metallic palladium was 0.25% by weight based on the weight of carrier.

2.2. Production and analysis of diethyl carbonate (DEC)

Catalytic activities were measured by a computer-controlled continuous micro reactor system (MRCS-8004B) with a stainless steel tubular reactor of 8 mm inner diameter. The reaction products collected by a cooling trap were taken out and sampled each hour, and analyzed by a gas chromatograph (GC) (4890D, Agilent) with a FID detector. The reaction conditions were steadily kept at a reaction temperature of 150 °C and a reaction pressure of 0.64 MPa.

2.3. Characterization of catalysts

Transmission electron microscopy (TEM) images were recorded with a Philips Tecnai G2 F20 operated at 200 kV. The surface area (BET method) and average pore diameter (BJH method) were determined by N_2 adsorption–desorption method by a Micromeritics-ASAP 2020. Pore size distribution was estimated from the adsorption branch of the isotherm by the BJH method. The characterization of catalysts was conducted by X-ray powder diffraction (XRD) using a Rigaku C/max-2500 diffractometer using graphite filtered Cu Kα radiation ($\lambda = 1.54056$ Å) at 40 kV and 200 mA with a scanning rate of $4^\circ\,min^{-1}$ from $2\theta = 1^\circ$ to $2\theta = 10^\circ$. X-ray photoelectron spectra (XPS) were recorded under ultra high vacuum ($<10^{-6}$ Pa) at a pass energy of 93.90 eV on a PerkinElmer PHI 5000C ESCA system equipped with a dual X-ray source by using Mg Kα (1253.6 eV) anode. Further elemental analysis was performed by inductively coupled plasma-atomic emission spectroscopy (ICP-AES) (VISTA-MPX) operated at high frequency emission power of 1.5 kW and plasma airflow of 15.0 L/min. Sample was dissolved in the mixture of HNO_3, HF and HBO_3, and then diluted with water. The IR spectroscopic measurements were carried out on a Nicolet, 5DX spectrometer with 4 cm^{-1} resolution and 400–4000 cm^{-1} scanning ranges.

3. Results and discussion

3.1. Characterization of HMS materials and catalysts

The binary catalyst systems $PdCl_2$-$CuCl_2$-TBAB employing mesoporous HMS silica as a support for the gas-phase oxidative carbonylation of methanol at atmospheric pressure have exhibited excellent catalytic performance in the reaction of dimethyl carbonate (DMC) synthesis [17]. HMS was reported to demonstrate more advantages than other supports, such as larger pores and higher thermal and hydrothermal stability [26]. However, the loss of the chlorine and the remodel of active copper species on the surface for this Wacker-type catalyst limited its development of the bimetallic HMS catalyst.

For this reason, it may be interesting to introduce transition metals into the framework of molecular sieve when preparing an oxidative carbonylation catalyst. Up to now, there have been no references about the use of Cu-substituted HMS as catalysts for DEC synthesis.

Fig. 1 showed the TEM images of the corresponding particle size distributions for Cu-HMS. TEM revealed that a mesoporous molecular sieves phase formed under the actual synthesis condition. The Cu-HMS support phase had a wormhole-type mesoporous structure with an amorphous framework, similar to previously reported mesoporous silica HMS [24].

The textural parameters of the samples were measured using the BET method by N_2 adsorption and desorption. The pore size of all samples was about 2.3–2.6 nm, similar to the case of ordered mesoporous silica HMS [24]. All samples exhibited BET specific surface area (S_{BET}) and framework-confined mesopore volumes (V_{pore}) in Table 1. It could be seen that the specific surface area decreased with introducing copper into the framework. It was considered that higher amounts of Cu incorporation reduced the surface area which could be ascribed to the decrease in hexagonal order as suggested by XRD measurements as follows.

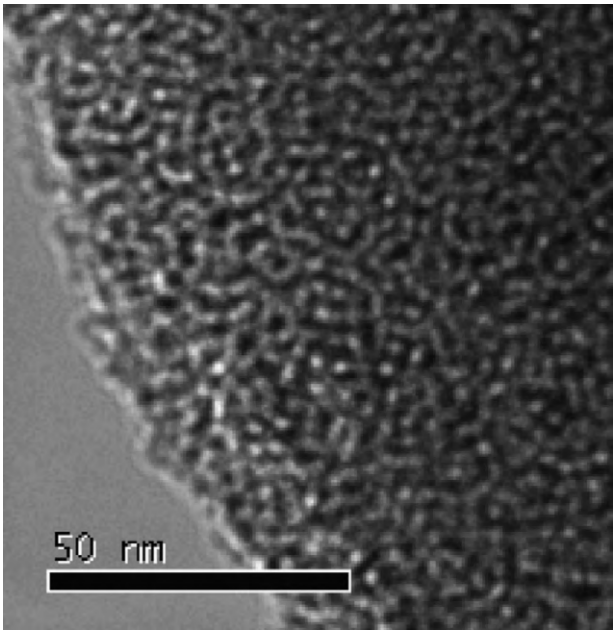

Fig. 1. TEM images of Cu-HMS.

Table 1
Textural properties of the samples.

Sample	S_{BET} ($m^2\ g^{-1}$)	V_{pore} ($cm^3\ g^{-1}$)	Pore size (nm)
HMS	1089	0.6085	2.42
Cu-HMS	832	0.5495	2.53
$PdCl_2$/Cu-HMS	788	0.5268	2.32

The fresh modified material Cu-HMS was also characterized by XPS and ICP techniques. Interestingly, no obvious signals of copper were detected from XPS analysis for all Cu-HMS samples, which might be caused by the copper embedment in framework of HMS. In turn, it leaded to the surface contents of copper species out of the detectable sensitivity of XPS.

Additionally, based on ICP experiments, the amount of copper contained in the samples was 1.796 wt.%, which was consistent with that of copper initially added into reactants. From ICP and XPS analysis, it could be concluded that it was hard for copper to adhere on HMS surface but easy to be incorporated into HMS frame. Furthermore, the characterization of the mesoporous molecular sieves still remained.

Another technique employed in this study to characterize Cu sites in mesoporous materials was infrared spectroscopy (FT-IR). As shown in Fig. 2, a band at 960 cm^{-1} was found in the spectra of Cu-HMS, which could be attributed to the Si-O stretching vibration of $SiO^{\delta-}...Tx^{\delta+}$ groups (Tx was the atom incorporated into the frame) [27]. The presence of the 960 cm^{-1} band in infrared spectra of Cu-HMS was also agreed with, at some point, the observations from XPS and ICP that Cu species were embedded in HMS frame.

3.2. Catalytic activities of $PdCl_2$/Cu-HMS

The catalytic results of $PdCl_2$/Cu-HMS catalysts on oxidative carbonylation of ethanol with CO and O_2 over $PdCl_2$/Cu-HMS catalysts were investigated. The bare Cu-HMS did not show any catalytic activities, which was similar to $PdCl_2$/HMS catalyst at the same reaction conditions.

The $PdCl_2$/Cu-HMS catalysts attracted much attention because of its high catalytic activities and the remarkable selectivity of 100% to DEC based on ethanol which the conversion of EtOH was about 4.8% and the STY of DEC was 110.5 g DEC L-cat^{-1} h^{-1}. Based on these results, we could draw a conclusion that Cu^{2+} species in the frame could not provide any active catalytic sites alone. It turned out that the existence of Pd^{2+} loaded on the surfaces of catalyst played a critical role in the DEC synthesis when Pd^{2+} facilitated

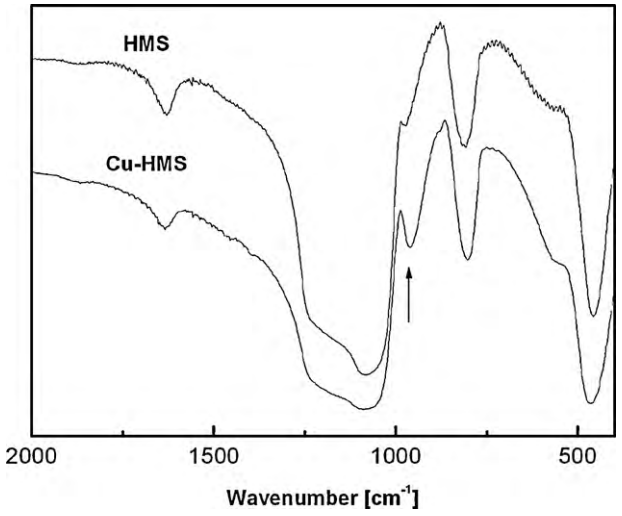

Fig. 2. Infrared spectra of HMS and Cu-HMS samples.

Table 2
Comparisons of Cu-HMS catalysts based on Cu-HMS with varying Si/Cu ratios on catalytic performances.[a]

Si/Cu ratios[b]	Conversion of EtOH (%)	STY of DEC (g L^{-1} h^{-1})	$S_{DEC/EtOH}$ (%)
10	2.5	65.7	100
20	3.6	97.8	100
50	4.8	110.5	100
75	4.2	105.6	100
100	2.9	77.2	100

[a] Reaction condition: T = 423 K, P = 0.64 MPa, O_2 = 10 sccm, CO = 80 sccm, N_2 = 50 sccm.
[b] Pd-loading = 0.25 wt.%.

Cu^{2+} in the frame to show the better activities. Therefore, it could be concluded that the main reasons that $PdCl_2$/Cu-HMS catalysts showed desirable catalytic activities probably was the interaction of surface loaded Pd^{2+} and Cu^{2+} in the frame.

3.3. Effect of Si/Cu ratio of Cu-HMS support

It is well known that the structures of support play an important role in the structures and activities of supported catalysts. The introduction of copper element not only promote more active centers also facilitate significant modification of the textural structures of HMS supports. In order to get better understanding of the influence of Si/Cu ratio, the catalytic results of $PdCl_2$/Cu-HMS catalysts based on Cu-HMS with varying Si/Cu ratios were also investigated in Table 2. The ethanol conversion and STY of DEC formation gradually increased at a low Si/Cu molar ratio, followed by a steep leveling off around Si/Cu > 50/1. The conversions of EtOH demonstrated the same trend as STY of DEC, and the selectivity based on EtOH to DEC was 100% all the time. An optimized Si/Cu molar ratio existed for catalytic activity, which was about 50/1. The results in Table 2 suggested that increasing Cu content in the Cu-HMS would improve catalytic reactivity in a certain extent but excess copper incorporated into HMS sample would result in collapse and disordered structures of the HMS framework.

The effect of different amount $PdCl_2$ on the catalyst activities was further investigated, as shown in the following Fig. 3. As shown in Fig. 3, the catalytic performance was improved sharply with the amount of Pd-loading increasing when the amount of Pd-loading was less than 0.25 wt.%. In addition, when the amount of Pd-loading was more than 0.25 wt.%, it was shown that $PdCl_2$/Cu-HMS catalysts have similar catalytic performance, which did not present the major difference of the effect of different amount Pd-loading. And the favorable amount of Pd-loading is 0.25 wt.%.

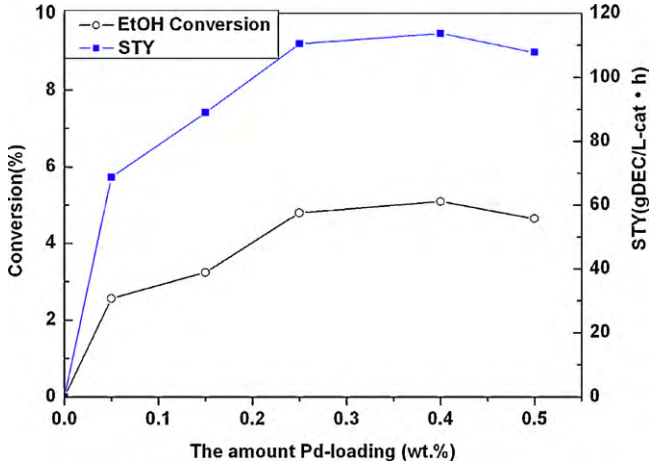

Fig. 3. The effect of different amount Pd on the catalyst activities.

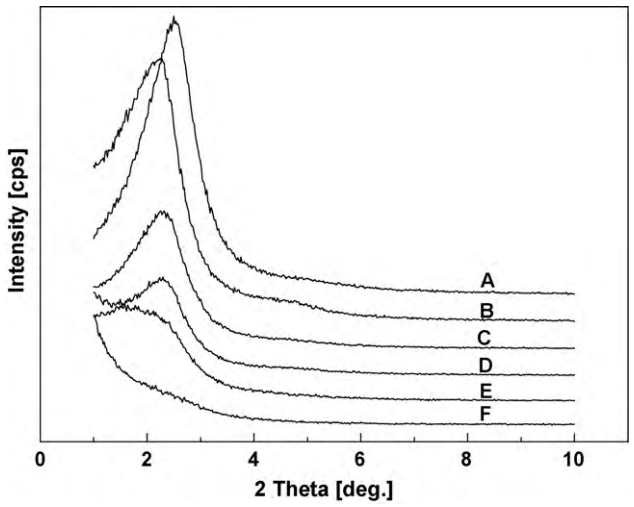

Fig. 4. XRD patterns of the Cu-HMS samples with different Si/Cu molar ratios. (A: Si/Cu = ∞, B: Si/Cu = 100, C: Si/Cu = 75, D: Si/Cu = 50, E: Si/Cu = 20, F: Si/Cu = 10).

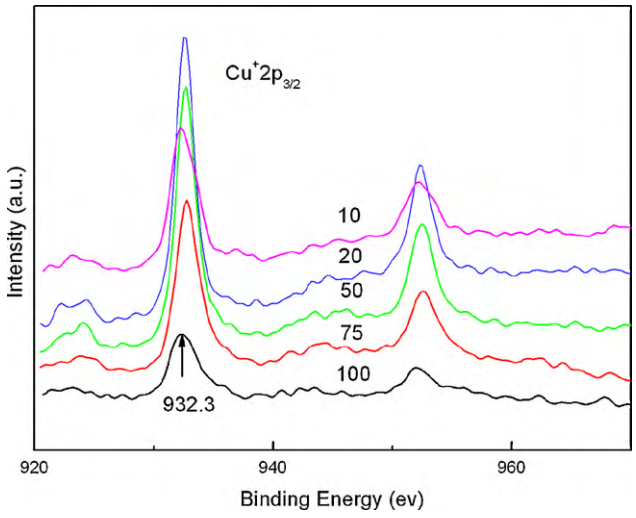

Fig. 5. Cu 2p XPS spectra of Cu-HMS samples with varying Si/Cu ratios.

Also, Cu-HMS materials with different Si/Cu ratios obtained after calcination were characterized by XRD and sorption techniques to establish the understanding of their structures and textures. The XRD patterns of Cu-HMS were shown in Fig. 4. Again, all XRD patterns of the samples were dominated by a peak around $2\theta < 3^\circ$ corresponding to the [1 0 0] diffraction, which was the only diffraction peak of Cu-HMS supports with different Si/Cu ratios. It could be noted that increasing Cu contents leaded to the decrease of d spacing while the intensity of the reflection peak [1 0 0] decreased slightly with more Cu in the frame of HMS. As a matter of fact, for the sample with Si/Cu = 10, we could not observe any XRD peaks in the low-angle range, implying a very disordered structure, which could be caused by the partial collapse of the HMS framework and reduction of hexagonal order because of the excess copper species incorporating into HMS sample.

Calculated through nitrogen physisorption experiments, the surface area (BET method) and average pore diameter (Barrett–Joyner–Halenda (BJH) method) are shown in Table 3. The Barrett–Joyner–Halenda method for calculating pore size distributions [28] is based on a model of the adsorbent as a collection of cylindrical pores. From Table 3, increasing Cu contents leaded to the decrease of surface area and the increase of pore diameter because of more Cu in the frame of HMS and the part blocking up the pore path of HMS. Cu-HMS (Si/Cu = 50) has a bigger pore diameter and higher surface area relatively. The bigger pore diameter can reduce the energy barrier and make the reactants enter the channel of catalyst easier. The higher surface area means more active center reacting with the reactants. All of these are beneficial to the catalytic performance. Thus, it shows a better catalytic performance using Cu-HMS (Si/Cu = 50) as catalyst support.

In order to gain an insight into the chemical state of the active components on the Cu-HMS with varying Si/Cu ratios, Cu $2p_{3/2}$ XPS analysis has been carried out. As shown in Fig. 5, The sample Cu-HMS (Si/Cu = 100) showed the principal Cu $2p_{3/2}$ line centered around 932.3 eV, which was assigned to Cu^+ cations [17,29,30]. And the Cu $2p_{3/2}$ peak of Cu-HMS (Si/Cu = 10) located at 932.9 eV. The Cu $2p_{3/2}$ peak of Cu-HMS shifted towards higher binding energy slightly and the intensity of that first increased and then slightly decreased with increasing Cu contents. It could be noted that increasing Cu contents leaded to increase of active copper species on the catalyst surface. In addition, it suggested excessive Cu adding did not disperse on the catalyst surface and blocked up the pore path of the Cu-HMS, which was in agreement with that the excess copper species leaded to partial collapse of the HMS framework and reduction of hexagonal order from XRD patterns. Because the existence of appropriate Cu^+ is related to the better catalytic activity [18,21], it could be easily explained that Cu-HMS (Si/Cu = 50) showed the better catalytic performances in our work.

To further explore the correlation of inherent structures of Cu-HMS with varying Si/Cu ratios and catalytic activities, infrared measurements were taken and the spectra of the samples were shown in Fig. 6. As seen, the bands characteristics of samples were quite similar. The intensity of the bands at 450 cm^{-1}, which could be interpreted as the tetrahedral vibration of zeolites [27], determined the crystal degree of mesoporous structures. It was supposed that the intensity of the bands at 450 cm^{-1} was the result of the interaction between active components and the support surface as well as blockage of the pore mouths by loading active species. The bands

Table 3
Comparisons of textural properties of Cu-HMS with varying Si/Cu ratios.

Si/Cu ratios	S_{BET} ($m^2\ g^{-1}$)	V_{pore} ($cm^3\ g^{-1}$)	Pore size (nm)
10	250	0.3078	3.37
20	465	0.4792	2.98
50	832	0.5495	2.53
75	858	0.5570	2.50
100	887	0.5785	2.47

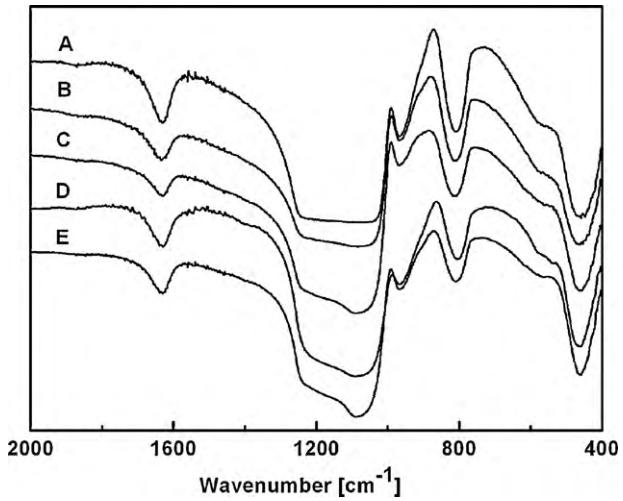

Fig. 6. IR spectra of the Cu-HMS samples with varying Si/Cu ratios. (A: Si/Cu = 10, B: Si/Cu = 20, C: Si/Cu = 50, D: Si/Cu = 75, E: Si/Cu = 100).

at 1080 and 1250 cm^{-1}, which could be ascribed to the Si–O–Si stretching vibration, significantly decreased with the increase of Cu contents. It was inferred that the relative weakening of the 1080 and 1250 cm^{-1} band might be attributed to the breakage Si–O–Si brands for Cu incorporation [27]. As also shown in Fig. 6, the presence of the 960 cm^{-1} band in the infrared spectra of samples might be regarded as a proof for Cu incorporation.

4. Conclusion

A novel catalyst, $PdCl_2$/Cu-HMS, for DEC synthesis was investigated in the gas-phase oxidative carbonylation of ethanol in this work which showed excellent catalytic performances. TEM, nitrogen sorption, XPS, ICP and IR analysis suggested that an ordered mesoporous Cu-HMS with large surface area and pore volume was successfully synthesized, and copper was incorporated into the Cu-HMS frame with favorable mesoporous stability. The improvement of the catalytic activities with the optimized Si/Cu molar ratio about 50 can be ascribed to both enough active sites and preferable order degree of mesoporous structures.

Acknowledgements

The financial supports from the National Natural Science Foundation of China (NSFC) (grant no. 20876112), and the Science Foundation for Youth of Jiangnan University (no. 2009LQN13) are gratefully acknowledged.

References

[1] M.A. Pacheco, C.L. Marshall, Energy Fuels 11 (1997) 2–29.
[2] J.W. Crandall, J.E. Deitzler, L.A. Kapicak, F. Poppelsdorf, U.S. Patent 4,663,477 (1987).
[3] J.S. Gnanaraj, E. Zinigrad, L. Asraf, M. Sprecher, H.E. Gottlieb, w. Geissler, M. Schmidt, D. Aurbach, Electrochem. Commun. 5 (2003) 946–951.
[4] M. Herstedt, M. Stjerndahl, T. Gustafsson, K. Edstrom, Electrochem. Commun. 5 (2003) 467–472.
[5] G. Moumouzias, G. Ritzoulis, D. Siapkas, D. Terzidis, J. Power Sources 122 (2003) 57–66.
[6] I.E. Muskat, F. Strain, U.S. Patent 2,379,250 (1941).
[7] U. Romano, R. Tessi, G. Ciprianni, L. Micucci, U.S. Patent 4,218, 391 (1980).
[8] X.B. Ma, M.M. Fan, P.B. Zhang, Catal. Commun. 5 (2004) 765–770.
[9] B.C. Dunn, C. Guenneau, S.A. Hilton, J. Pahnke, E.M. Eyring, J. Dworzanski, H.L.C. Meuzelaar, J.Z. Hu, R.J. Pugmire, Energy Fuels 16 (2002) 177–181.
[10] Z. Zhang, X.B. Ma, J. Zhang, F. He, S.P. Wang, J. Mol. Catal. A: Chem. 227 (2005) 141–146.
[11] N.S. Roh, B.C. Dunn, E.M. Eyring, R.J. Pugmire, H.L.C. Meuzelaar, Fuel Process. Technol. 83 (2003) 27–38.
[12] T.C. Liu, C.S. Chang, Appl. Catal. A: Gen. 304 (2006) 72–77.
[13] P.T. Anastas, J.C. Warner, Green Chemistry: Theory and Practice, Oxford University Press, London, 1998, p. 11.
[14] I.Z. Nadolska, K. Warmuzinski, J. Richter, Catal. Today 114 (2006) 226–230.
[15] K. Tomishige, T. Sakaihori, Y. Ikeda, K. Fujimoto, Catal. Lett. 58 (1999) 225–229.
[16] J.Y. Ryu, U.S. Patent 5,902,894 (1999).
[17] P. Yang, Y. Cao, J.C. Hu, W.L. Dai, K.N. Fan, Appl. Catal. A: Gen. 241 (2003) 363–373.
[18] S.T. King, J. Catal. 161 (1996) 530–538.
[19] S.T. King, Catal. Today 33 (1997) 173–182.
[20] Z. Li, K.C. Xie, R. Slade, Appl. Catal. A: Gen. 205 (2001) 85–92.
[21] M. Richter, M.J.G. Fait, R. Eckelt, E. Schreier, M. Schneider, M.-M. Pohl, R. Fricke, Appl. Catal. B 73 (2007) 269–281.
[22] I.J. Drake, Y.H. Zhang, D. Briggs, B. Lim, T. Chau, A.T. Bell, J. Phys. Chem. B 110 (2006) 11654–11664.
[23] P.B. Zhang, Z. Zhang, S.P. Wang, X.B. Ma, Catal. Commun. 8 (2007) 21–26.
[24] P.T. Tanev, T.J. Pinnavaia, Science 267 (1995) 865–867.
[25] T.R. Pauly, T.J. Pinnavaia, Chem. Mater. 13 (2001) 987–993.
[26] P.T. Tanev, T.J. Pinnavaia, Chem. Mater. 8 (1996) 2068–2079.
[27] R. Szostak, Molecular Sieves, 2nd ed., Blackie Academic & Professional, London, 1998, pp. 234, 240.
[28] E.P. Barrett, L.G. Joyner, P.P. Halenda, J. Am. Chem. Soc. 73 (1951) 373–380.
[29] F. Garbassi, G. Petrini, J. Catal. 90 (1984) 113–118.
[30] W.L. Dai, Q. Sun, J.F. Deng, D. Wu, Y.H. Sun, Appl. Surf. Sci. 177 (2001) 172–179.